2024-03-16

# Maximizing EV Profit and Grid Stability Through Virtual Power Plant Considering V2G

A. Selim Türkoğlu

H. Cihan Güldorum

Ibrahim Sengor

Energy Reports 11 (2024) 3509–3520

Contents lists available at ScienceDirect

Energy Reports

journal homepage: www.elsevier.com/locate/egyr

Research paper

# Maximizing EV profit and grid stability through Virtual Power Plant considering V2G☆

A. Selim Türkoğlu [a], H. Cihan Güldorum [a,b], Ibrahim Sengor [c,*], Alper Çiçek [d], Ozan Erdinç [a], Barry P. Hayes [e,f]

[a] Department of Electrical Engineering, Faculty of Electrical and Electronic Engineering, Yildiz Technical University, Istanbul, 34220, Türkiye
[b] Escuela Técnica Superior de Ingeniería Industrial, Universidad de Castilla-La Mancha, Ciudad Real, 13071, Spain
[c] Department of Electrical and Electronic Engineering, Munster Technological University, Cork, T12 P928, Ireland
[d] Department of Electrical and Electronics Engineering, Faculty of Engineering, Trakya University, Edirne, 22030, Türkiye
[e] MaREI, the SFI Research Centre for Energy, Climate and Marine, University College Cork, Cork, T12 K8AF, Ireland
[f] School of Engineering and Architecture, University College Cork, Cork, T12 K8AF, Ireland

ARTICLE INFO

*Keywords:*
Electric vehicle
Optimal power flow
Vehicle-to-grid
Virtual power plant

ABSTRACT

The electrification of transportation through the widespread adoption of electric vehicles (EVs) has raised substantial concerns within the realm of power grid operations. This concern predominantly stems from the elevated electricity demand brought about by the surging population of EVs, consequently exerting strain on the power grid infrastructure which can be reduced with vehicle-to-grid (V2G) technology integration. To address this issue, this paper delves further into the realm of grid integration by introducing a Virtual Power Plant (VPP) concept to enhance the synergy between EVs and power grid. This study aims to compare different realistic objectives, ranging from total active power loss and voltage drop minimization to EV profit maximization and then optimize the balance between the distribution grid power quality and VPP profit through bi-level modeling. The presented model is devised as mixed-integer quadratically constrained programming (MIQCP) and incorporates Temporal Convolutional Network (TCN) based forecasting to handle the uncertain behavior of the residential loads using historical data. The experiments are conducted in IEEE 33-Bus and real-world 240-Bus distribution networks. The results indicate that enabling bidirectional power flow between the grid and VPP can yield significant profits for EV users while only marginally impacting the active power loss, approximately around 5%. This validation underscores how V2G not only presents various advantages for power system operators but also benefits EV users simultaneously.

## 1. Introduction

### 1.1. Motivation and background

The transportation sector is one of most significant contributor to carbon emissions, accounting for around 37% of global emissions (IEA, 2022). In recent years, there has been increasing awareness of the need to address climate change and reduce carbon emissions, leading to a growing interest in electrified transportation. Electric vehicles (EVs) offer a promising solution for reducing emissions and improving energy efficiency, and advances in EV technologies have made them increasingly viable for an extensive variety of applications. Consumer behavior and government incentives also fulfill a crucial function in the adoption of electrified transportation (Wang et al., 2017; Dutta and Hwang, 2021).

However, the broad acceptance of EVs also brings new challenges for grid integration and the management of power systems. Uncoordinated EV demand may result with significant peaks in electricity consumption, which can stress the power network and lead to increased costs and reduced reliability. Coordinated charging strategies have emerged as effective means to minimize the negative impacts of

☆ The work of I. Sengor was supported by Science Foundation Ireland (SFI) under Grant No. 12/RC/2302_P2. The work of B.P. Hayes was supported by the Department of Business, Enterprise, and Innovation, under the Government of Ireland's Project 2040 Plan ("CENTS" project, contract DT 2018 0040-D). The work of Ozan Erdinc was supported by Turkish Academy of Sciences (TUBA) under Distinguished Young Scientist Program (GEBIP). The work of H. C. Güldorum was supported in part by Grant SBPLY/21/180501/000154 funded by the Junta de Comunidades de Castilla-La Mancha and by the ERDF, and in part by Grant 2023-GRIN-34074 funded by the University of Castilla-La Mancha.

* Corresponding author.
*E-mail address:* Ibrahim.Sengor@mtu.ie (I. Sengor).

https://doi.org/10.1016/j.egyr.2024.03.013
Received 5 January 2024; Received in revised form 26 February 2024; Accepted 6 March 2024
Available online 16 March 2024

**Nomenclature**

The sets and indices, parameters, and variables used throughout the study are stated below.

**Sets and Indices**

| | |
|---|---|
| $h$ | Set of electric vehicles. |
| $i, j$ | Set of buses. |
| $t$ | Set of time periods. |

**Parameters**

| | |
|---|---|
| $\Delta T$ | Time granularity. |
| $A, B, C$ | Binary parameter for objective selection. |
| $CE_{i,h}^{EV}$ | Charging efficiency of EV $h$ connected to bus $i$ [%]. |
| $CR_{i,h}^{EV}$ | Charging rate of EV $h$ connected to bus $i$ [kW]. |
| $D^{VPP}$ | Reference profit of the VPP. |
| $DE_{i,h}^{EV}$ | Discharging efficiency of EV $h$ connected to bus $i$ [%]. |
| $DR_{i,h}^{EV}$ | Discharging rate of EV $h$ connected to bus $i$ [kW]. |
| $L^{VPP,max}$ | Maximum allowable profit of the VPP. |
| $L^{VPP,min}$ | Minimum allowable profit of the VPP. |
| $P_{i,t}^{Demand}$ | Active power demand of bus $i$ in period $t$ [pu]. |
| $Q_{i,t}^{Load}$ | Reactive power load of bus $i$ in period $t$ [pu]. |
| $R_{i,j}$ | Resistance of branch $(i, j)$ [pu]. |
| $S_{i,j}^{Max}$ | Maximum branch capacity $(i, j)$ [pu]. |
| $SoE_{i,h}^{EV,des}$ | Desired SoE of EV $h$ [kWh]. |
| $SoE_{i,h}^{EV,init}$ | Initial SoE of EV $h$ [kWh]. |
| $SoE_{i,h}^{EV,max}$ | Maximum SoE of EV $h$ [kWh]. |
| $SoE_{i,h}^{EV,min}$ | Minimum SoE of EV $h$ [kWh]. |
| $T_{i,h}^{a}$ | Arrival time of EV $h$. |
| $T_{i,h}^{d}$ | Departure time of EV $h$. |
| $V_{i}^{max}$ | Maximum voltage of bus $i$ [pu]. |
| $V_{i}^{min}$ | Minimum voltage of bus $i$ [pu]. |
| $X_{i,j}$ | Reactance of branch $(i, j)$ [pu]. |

**Decision Variables**

| | |
|---|---|
| $\Lambda$ | Lagrange function. |
| $\lambda_1, \lambda_2, \lambda_3, \lambda_4$ | Lagrange multipliers for the KKT conditions. |
| $f_{i,j,t}^{active}$ | Active power flow of branch $(i, j)$ in period $t$ [pu]. |
| $f_{i,j,t}^{reactive}$ | Reactive power flow of branch $(i, j)$ in period $t$ [pu]. |
| $I^{VPP}$ | Total profit of the VPP. |
| $K^{VPP}$ | Profit loss of the VPP. |
| $P_{i,h,t}^{EV,ch}$ | Charging power of EV $h$ in period $t$ [kW]. |
| $P_{i,h,t}^{EV,dis}$ | Discharging power of EV $h$ in period $t$ [kW]. |
| $P_{i,j,t}^{Loss}$ | Active power losses of branch $(i, j)$ in period $t$ [pu]. |
| $P_{i,t}^{gen}$ | Total active power transferred from the substation bus $i$ in period $t$ [pu]. |
| $P_{i,t}^{Load}$ | Active power load of bus $i$ [pu]. |
| $Q_{i,j,t}^{Loss}$ | Reactive power losses of branch $(i, j)$ in period $t$ [pu]. |
| $Q_{i,t}^{gen}$ | Total reactive power transferred from the substation bus $i$ in period $t$ [pu]. |
| $SoE_{i,h,t}^{EV}$ | SoE of EV $h$ in period $t$ [kWh]. |
| $u_1^{aux}, u_2^{aux}, u_3^{aux}, u_4^{aux}$ | Auxiliary binary variables for the big M notation. |
| $V_{i,t}^{Bus}$ | Voltage of bus $i$ in period $t$ [pu]. |

EVs. Furthermore, vehicle-to-grid (V2G) technology offers benefits to address these challenges such as integrating EVs into the power grid and providing valuable grid services, including frequency regulation, energy storage, and load balancing (Sengor et al., 2020).

V2G technology enables EVs to engage with the power grid via either discharging or charging their batteries based on the grid's demand for power as a form of a Virtual Power Plant (VPP). This approach has the potential to contribute valuable utility services, like energy storage, load balancing and frequency regulation (Sengor et al., 2020). The use of V2G technology can help to address the challenges posed by uncoordinated EV charging, which can lead to significant peaks in electricity demand and stress on the power grid. By utilizing V2G technology, EVs can function as mobile energy storage units, enabling the power grid to better manage fluctuations in demand and supply. Furthermore, V2G technology holds the promise of delivering financial advantages to both EV owners and grid operators, by allowing users to trade excess energy back to the grid and providing grid operators with key grid operations (Anon, 2023b). However, there are still economic and technical hurdles that must be addressed in order to fully realize the potential of V2G technology, and further research is needed to develop more sophisticated algorithms and protocols for managing V2G systems.

### 1.2. Literature review

In recent years, the integration of V2G technology into distribution systems (DSs) have attracted considerable interest in the research community.

Mazumder and Debbarma (2021) investigated the use of the metaheuristic optimization technique known as the water cycle algorithm (WCA) to minimize the peak-to-average ratio and charging prices, while also maximizing the penetration level of EVs. This paper modeled EV chargers as reactive power compensating devices to alleviate voltage deviations, using IEEE 33-bus DS. However, the active times of EVs, battery capacity and the charging/discharging efficiency were assumed fixed. Mehta et al. (2019) introduced a multiyear hybrid planning method applying a genetic algorithm (GA) with sample aging to minimize the peak-to-average ratio and total daily cost in a power grid. The optimization process consisted of the expenses related to infrastructure upgrades and power losses, and satisfying the energy requirements of EVs. The study created 100 scenarios annually to evaluate the performance of the suggested algorithm. Haq et al. (2022) introduced a game theoretic approach to minimize the alteration in injected power at each node, with the objective of addressing congestion issues while preserving power equilibrium in the network. The paper focused on resolving congestion in the system and maintaining stability while meeting the power demand. Singh and Tiwari (2020) proposed a genetic algorithm to optimize power dispatch with the aim of minimizing power losses in the network while employing V2G operation. The paper also conducted a cost-benefit assessment of the EV arranging scenarios and evaluated the impact of grid reconfiguration on system operation and planning. The paper considered the EVs' state-of-charge (SoC), battery capacity, (dis)charging efficiency and trip conditions in the optimization process. Guo et al. (2020) suggested a mixed-integer quadratic programming

(MIQP) to efficiently manage the charging and discharging considering a network reconfiguration. The paper developed a model to quantify the aggregated energy availability and charging demand from EVs in traffic equilibrium, considering their travel plans and individual utility, and connects the traffic pattern with the spatial–temporal distribution of electricity demand. The objective of the paper was to achieve optimal coordination between EV charging/discharging and dynamic distribution network reconfiguration. Mehrabi et al. (2020) suggested a two-step mixed-integer nonlinear programming (MINLP) via greedy-based algorithm to maximize the combined revenue of both the supply and demand sides. Their optimization process considered practical expenses for EV batteries, upkeep and workforce costs, as well as real-time pricing. The paper included the amount of charging stations (CSs), EV activity times, and the likelihood of V2G penetration. Huang (2019) devised an interior point optimization approach using a sensitivity method to minimize the cost associated with charging/discharging and the battery degradation cost resulting from V2G operations, as well as maximize local peak load shifting in a power system. During the optimization process, the bulk of the nonlinear constraints was converted into linear constraints and reduced the amount of equations. The paper considered two strategies: cost-reduction strategy and peak-shifting strategy. The study used a three-phase power flow model and explicitly considered EV owner convenience. In Zhang et al. (2022), a wind power curtailment strategy using EVs is proposed using particle swarm optimization algorithm. This strategy aims to reduce wind curtailment, improve wind power consumption rate, and minimize output fluctuation and amplitude. In the model, EV aggregators set charging tariffs, and a multi-objective optimization function is established to integrate wind power curtailment consumption and minimize output fluctuation. However, they did not integrated their system to DS by modeling power flow constraints. Dhawale et al. (2024), a system that integrates renewable power generation with conventional and plug-in EVs to meet power demand is presented. It tests this system using chaotic arithmetic optimization algorithms to minimize generation costs. The study contributes to scheduling power generation effectively and minimizing operating costs in varied-unit systems addressing security constraints and unit commitment issues. However, it only considered the relationship among the power generation and consumption. No detailed modeling was taken into account. In Rajani and Kommula (2022), a hybrid strategy for managing energy in EV charging station (EVCS) and DS using Giza Pyramids Construction (GPC) and recalling-enhanced recurrent neural network (RERNN) is presented. Their goal was to maximize energy use, minimize system costs, and reduce voltage deviation and power loss. The GPC approach is used to analyze energy interaction, bidirectional trading, solar uncertainty, and cost analysis based on selling energy. But they did not modeled DS explicitly. While many studies have examined different aspects of V2G technology, the aforementioned papers have not explicitly considered the AC optimal power flow (OPF) constraints.

Velamuri et al. (2022) developed a model that uses the grasshopper optimization (GO) algorithm to reduce power loss and peak-to-average ratio in a distribution system. The optimization process involved three modes, including the first in first out (FIFO) mode for grid-to-vehicle (G2V) charging, a scheduled mode for smart G2V charging, and a comparison of V2G modes. The paper's objective was to assess the GO algorithm's efficiency across various operational modes. Kazemtarghi et al. (2022) examined the current summation method that uses EVs to improve the frequency stability of the DS. The research examined how bidirectional charging of EVs influenced frequency stability, voltage profile and power quality, within the power network. The paper introduced a comprehensive model of a real-world bidirectional onboard charger designed to assess the frequency distortion in the line current induced by EVs. The study takes into consideration diverse EV power levels, operational modes and voltage levels. Ahmed et al. (2021) developed a coordination scheme based on distributed controllers for managing the impact of EV power on the DS by using quadratic programming with interior point method and the pattern search algorithm (PSA). The scheme aimed to improve the voltage profile within a grid, reduce the total power as well as the total charging costs and demand fluctuations, while considering unpredictable arrivals/departures and the preferred charging time windows of EVs with V2G technology. The study used actual residential loads recorded in Australia and focused on minimizing fluctuations in power demand and the overall energy expenditure. Zhang and Leung (2022) presented a hierarchical system model to enhance V2G scheduling and power flow for providing regulatory services. The paper first formulated the OPF problem at the grid level by incorporating power flow routers within the network. The model was transformed into a convex problem by employing semidefinite programming relaxation, and the complexity of the system network was further reduced using the tree decomposition method. After addressing the grid-level problem, a scheduling problem based on forecasts was developed at the EV level to coordinate EVs in providing V2G regulatory services. An online scheduling problem was then formulated to cope with forecast uncertainties. Decentralized algorithms were developed to manage the schedules of EVs, making it possible to address these issues easily scalable. The paper used a fixed EV type and assumed there no household load. Kwon et al. (2020) employed the mixed-integer linear programming (MILP) algorithm; the aim was to minimize the overall cost resulting from energy losses. This was achieved subject to the predictions of load demand and traffic congestion for the following day. The research focused on managing the energy costs of an EVCS and the optimization of the energy distribution within the system to reduce costs. Deb et al. (2020) proposed a novel strategy by using particle swarm optimization (PSO) to achieve maximum penetration of EVs while minimizing the overall cost in a photovoltaic (PV) powered grid system. The optimization process included the forecasting of SoC of EV batteries using gradient boosting regression trees. In the model, it was required that EVs should be connected for at least four hours and their charging/discharging power was assumed fixed and 2 kW. Nizami et al. (2021) analyzed a multi-agent system architecture using mixed-integer programming (MIP) to minimize the electricity expenditure for EV owners in DS. The optimization process included an improved bidding model to facilitate the interaction between EV owners and the electricity market. The study focused on a low voltage grid in Australia, with real demand and EV records. The paper aimed to assess the effectiveness of the suggested multiagent system architecture and bidding model in practical scenarios. Archana and Rajeev (2021) proposed a novel EV placement index to determine the maximum threshold score for siting EVCS in different buses in a DS. The objective of the paper was to find a appropriate siting of EVCS in a DS while sustaining system performance in terms of power quality, reliability and voltage stability. Birk Jones et al. (2022), simulates 10 distribution feeders with predicted 2030 EV adoption levels to understand the impact of time of use (TOU) pricing on EV charging. It models multiple power systems to define power profiles, voltages, and line loading. The study also explores the impacts of TOUs on future integration scenarios and quantifies EV charging impacts on different load types. This paper considered power flow using OpenDSS, but did not modeled DS explicitly and demand response (DR) is not considered. It was rather than a simulation than an optimization. In Hasanien et al. (2023), introduces a novel Enhanced Coati Optimization Algorithm (ECOA) for optimal solutions of probabilistic OPF problems. The model uses metaheuristic optimization algorithm incorporating EVs in power systems. The approach is tested on IEEE-57 and IEEE-118 networks, demonstrating its effectiveness compared to other metaheuristic-based methods. Real wind speed, solar irradiance, and EV profiles are included in dynamic analyses. Nevertheless, the paper did not consider the effect of the residential loads and EV user preferences. Eid et al. (2022), optimizes DSs for renewable energy sources like solar and wind units, with existing EVCS connected to specific locations. Battery Energy Storage (BES) are provided at these

units, aiming to control power flow and enhance performance by minimizing fitness functions. The Gorilla Troop Optimizer (GTO) algorithm is used to solve the optimization problem, minimizing power loss and total voltage deviation. The GTO algorithm involves two stages: finding ideal solar and wind power unit positions and sizes, and optimizing BES operation after integrating EVCS. Yet, they did not aimed economical effects, EV user preferences and residential loads. In Aghajan-Eshkevari et al. (2023), a two-stage framework for optimizing EVs in the DS is proposed. The first stage considers EV mobility in the transportation system using the trip chain method and Dijkstra algorithm. The second stage focuses on optimal active and reactive power exchange with the distribution grid using a MILP model. The model considers both EV owners' and distribution network operator's benefits and includes the EV battery degradation cost. The framework is implemented on a standard IEEE 33-bus system and 30-node transportation network. However, the feasibility of the model was not tested with large-scale DS and crowd EV penetration. In conclusion, while many studies have examined various aspects of V2G technology, such as bidirectional power flow, coordinated charging strategies, and the provision of grid services, few have focused primarily on OPF models. Nonetheless, these models are crucial for accurately representing the behavior of the power system and determining the optimal dispatch of power to meet demand while minimizing costs and satisfying various operational constraints.

Despite the presence of numerous valuable studies in the literature, only Velamuri et al. (2022) and Kwon et al. (2020) considered power loss, but they did not focus on voltage and cost objectives. Although (Kazemtarghi et al., 2022; Ahmed et al., 2021; Zhang and Leung, 2022) and (Archana and Rajeev, 2021) analyzed voltage deviation, they did not target power loss effects. Zhang et al. (2022), Aghajan-Eshkevari et al. (2023) and Eid et al. (2022) modeled multi-objective approach, yet they did not developed a comprehensive approach. Overall, no comparative analysis has been conducted to evaluate the performance of V2G-enabled models that focus on active power loss reduction, voltage minimization, and EV user profit maximization, as well as forecasting residential loads with large-scale EV penetration across various distribution test systems. Moreover, the multi-objective models, which consider both the grid's power quality and user profit, did not gain enough attention.

### 1.3. Contributions and organization

In this study, the development of a V2G-enabled distribution grid that effectively addresses both grid constraints and EV user preferences are proposed. To accomplish this, a bidirectional EV scheduling model that optimizes multiple realistic objectives is proposed. Moreover, deep-learning-based forecasting technique is integrated to accurately capture the uncertain behavior of residential power to assist day-ahead load scheduling. By adopting these approaches, this paper makes significant contributions in developing a V2G-enabled distribution grid, introducing a comprehensive optimization model, leveraging load forecasting, and demonstrating the practical applicability of the proposed solutions. Furthermore, a key aspect of this research involves the concept of a VPP. By treating V2G infrastructure as a VPP, this study effectively harnesses the distributed energy resources within the EV fleet, enabling them to act as controllable and dispatchable assets. The research not only advances the field of energy optimization but also provides valuable insights for the sustainable integration of EVs into the power grid. The contribution of this paper is threefold:

- A comprehensive Mixed-Integer Quadratically Constrained (MIQCP) model is introduced to optimize the operation of V2G-enabled EV parking lots (EVPLs). This model takes into account various realistic objectives, such as active power losses, charging costs, and voltage deviations. It considers both EV and distribution system constraints, ensuring a holistic approach to grid optimization. Furthermore, this paper offers a bi-level modeling approach, balancing grid power quality and EV profit at the same time.
- The practical applicability of models is validated by conducting extensive testing on a large-scale system with a high number of EVs. By comparing the results under multiple scenarios, the scalability and real-world implementation potential of our proposed solutions are demonstrated. This empirical evidence strengthens the credibility and effectiveness of our approach in practical settings.
- A Temporal Convolutional Network (TCN) based forecasting is employed for residential load analysis. This technique enables us to capture the uncertain behavior of residential loads that are connected to buses. By leveraging TCNs, the day-ahead scheduling capabilities are enhanced, and more robust solutions are provided.

The work is unique in that it not only compared multiple objectives, but also forecasted residential load and tested it on various and large-scale systems, providing valuable insights into the optimization of EVPLs in a sustainable and efficient manner. The rest of the paper is organized as follows: The mathematical model of the bidirectional EV scheduling problem is given in Section 2. Case studies, simulations and related results obtained from both forecasting and optimization are examined in Section 3. Finally, the concluding remarks are evaluated in Section 4.

## 2. Methodology

### 2.1. Mathematical model of the VPP

The first part of the proposed model seeks to optimize the objective function by minimizing one of the following: the cumulative active power losses across branches, average voltage drop at the nodes, or EV-related costs, as specified in Eq. (1). Eq. (2) is the objective selector where A, B and C are the binaries and it helps to select only one objective during each model duration exclusively. Thus, the system can be operated targeting a different objective function each time, depending on different needs.

$$\begin{aligned} min\ & A \cdot \sum_i \sum_j \sum_t P_{i,j,t}^{loss} + B \cdot \sum_i \sum_t \overline{|V_0 - |V_{i,t}||} \\ & + C \cdot \sum_i \sum_h \sum_t \left( P_{i,h,t}^{EV,ch} - P_{i,h,t}^{EV,dis} \right) \cdot Price_t \end{aligned} \tag{1}$$

$$A + B + C = 1 \tag{2}$$

Eqs. (3) and (4) present the active and reactive power balance. The sum of power generated from the substation bus and power passes through the line must equal the total power demand in the node and the power losses in the line. The power losses, which are contingent on the power quantity transmitted through the line, can be calculated with a simplified model of "$I^2 * R$" loss in quadratic terms by using (5) and (6), respectively.

$$P_{i,t}^{gen} + \sum_{j \Omega_l^j} f_{i,j,t}^{active} - \sum_{j \Omega_l^i} f_{i,j,t}^{active} = P_{i,j,t}^{loss} + P_{i,t}^{load} \tag{3}$$

$$Q_{i,t}^{gen} + \sum_{j \Omega_l^j} f_{i,j,t}^{reactive} - \sum_{j \Omega_l^i} f_{i,j,t}^{reactive} = Q_{i,j,t}^{loss} + Q_{i,t}^{load} \tag{4}$$

$$P_{i,j,t}^{loss} = R_{i,j} \cdot \frac{(f_{i,j,t}^{active})^2 + (f_{i,j,t}^{reactive})^2}{V_0^2} \tag{5}$$

$$Q_{i,j,t}^{loss} = X_{i,j} \cdot \frac{(f_{i,j,t}^{active})^2 + (f_{i,j,t}^{reactive})^2}{V_0^2} \tag{6}$$

$$-S_{i,j}^{max} \le f_{i,j,t}^{active} \le S_{i,j}^{max} \tag{7}$$

$$-S_{i,j}^{max} \le f_{i,j,t}^{reactive} \le S_{i,j}^{max} \tag{8}$$

The viable space for the active branch power and reactive branch power is defined by (7) through (10), which consider the quadratic

terms to ensure that it does not exceed the transmission line's capacity. These constraints are essential to prevent overloading and secure the dependable functioning of the DS. In addition to (7)–(8), (9)–(10) defines the apparent power flow and considers the collective impact of both active and reactive power. Eq. (11) establishes the lower and upper thresholds of the voltage magnitude in the system while (12) is used to determine the voltage difference between neighboring buses which is derived from a comprehensive power system modeling perspective. The square terms in the equation capture the non-linear behavior of power losses, enhancing the precision of the voltage drop estimation in the transmission line. Furthermore, (13) asserts that the total load of bus i is equivalent to the demand of the bus plus the aggregate charging power from EVPL at the associated bus.

$$-\sqrt{2}\,S_{i,j}^{max} \le f_{i,j,t}^{active} + f_{i,j,t}^{reactive} \le \sqrt{2}\,S_{i,j}^{max} \tag{9}$$

$$-\sqrt{2}\,S_{i,j}^{max} \le f_{i,j,t}^{active} - f_{i,j,t}^{reactive} \le \sqrt{2}\,S_{i,j}^{max} \tag{10}$$

$$V_i^{min} \le V_{i,t}^{bus} \le V_i^{max} \tag{11}$$

$$V_{j,t}^{bus} = V_{i,t}^{bus} - \frac{R_{i,j}\cdot f_{i,j,t}^{active} + X_{i,j}\cdot f_{i,j,t}^{reactive}}{V_0} + \left(R^2+X^2\right)\cdot\frac{(f_{i,j,t}^{active})^2 + (f_{i,j,t}^{reactive})^2}{2V_0^3} \tag{12}$$

$$P_{i,t}^{load} = P_{i,t}^{demand} + \sum_i\sum_h\sum_t\left(P_{i,h,t}^{EV,ch} - P_{i,h,t}^{EV,dis}\right) \tag{13}$$

Eq. (14)–Eq. (18) represents the mathematical representation of the EV. Eq. (14)–Eq. (15) ensure that the charging and discharging power do not surpass the power threshold of the corresponding EV. Inequality (16) ensures that the EV charging procedure occurs safely within a predetermined lower and upper state-of-energy (SoE) range. Eq. (17) delineates the connection between the SoE and the charging/discharging rates of the EV throughout the parking duration. To prevent the EV's discomfort in terms of energy shortage, (18) denotes the attainment of the targeted SoE value at the time of departure. Eq. (19) specifies the initial SoE value of the EV upon arrival.

$$0 \le P_{i,h,t}^{EV,dis} \le DR_{i,h}^{EV,dis}, \quad \forall\, i,h,t \in \left(T_{i,h}^{a}, T_{i,h}^{d}\right] \tag{14}$$

$$0 \le P_{i,h,t}^{EV,ch} \le CR_{i,h}^{EV,ch}, \quad \forall\, i,h,t \in \left(T_{i,h}^{a}, T_{i,h}^{d}\right] \tag{15}$$

$$SoE_{i,h}^{EV,min} \le SoE_{i,h,t}^{EV} \le SoE_{i,h}^{EV,max}, \quad \forall\, i,h,t \in \left[T_{i,h}^{a}, T_{i,h}^{d}\right] \tag{16}$$

$$SoE_{i,h,t}^{EV} = SoE_{i,h,t-1}^{EV} + P_{i,h,t}^{EV,ch}\cdot CE_{i,h}^{EV,ch}\cdot\Delta T - \frac{P_{i,h,t}^{EV,dis}}{DE_{i,h}^{EV,dis}}\cdot\Delta T, \quad \forall\, i,h,t \in \left(T_{i,h}^{a}, T_{i,h}^{d}\right] \tag{17}$$

$$SoE_{i,h,t}^{EV} = SoE_{i,h}^{EV,des}, \quad \forall\, i,h \;\; if \;\; t = T_{i,h}^{d} \tag{18}$$

$$SoE_{i,h,t}^{EV} = SoE_{i,h}^{EV,init}, \quad \forall\, i,h \;\; if \;\; t = T_{i,h}^{a} \tag{19}$$

### 2.2. The enhanced bi-level model for the VPP

In this section, the bi-level model for the VPP that captures the balance between the distribution grid power quality and EVPL profit is proposed. Within this framework, the objective function of the upper level is minimizing the total active power loss whereas the lower model tries to maximizes its profit. To accomplish this, the previous equations were considered in the upper level, The first objective is determined as upper-level objective and for the lower-level, the reverse of the third objective is formulated in (20) since the goal is maximizing the EV profit.

$$I^{VPP} = \sum_i\sum_h\sum_t\left(P_{i,h,t}^{EV,dis} - P_{i,h,t}^{EV,ch}\right)\cdot Price_t \tag{20}$$

Additionally, the following constraints were created in the context of the bi-level model:

This bi-level optimization problem, as described in Eqs. (21)–(24), encompasses the costs and constraints for a VPP. Eq. (21) consists of inequalities related to reference values, revenue, and loss constraints for the VPP. The lower bound for revenue for the VPP is determined by (23), while the upper bound is determined by (24). Eq. (22) defines non-negative constraints for losses.

$$D^{VPP} - I^{VPP} - K^{VPP} \le 0 \quad \forall\lambda_1 \tag{21}$$

$$-K^{VPP} \le 0 \quad \forall\lambda_2 \tag{22}$$

$$L^{VPP,min} - I^{VPP} \le 0 \quad \forall\lambda_3 \tag{23}$$

$$I^{VPP} - L^{VPP,max} \le 0, \quad \forall\lambda_4 \tag{24}$$

In a normal optimization problem, it is not possible to optimize two objective functions at the same time. In this regard, to incorporate the lower-level problem within the framework of the upper-level problem, the lower-level problem has been transformed to Karush-Kuhn–Tucker (KKT) optimality conditions. To achieve this, the Lagrange function of the optimization problem presented in Eq. (25) was initially constructed to establish the KKT conditions. It should be noted that the KKT conditions consist of stationarity, complementarity slackness, dual feasibility, and primal feasibility conditions. The stationarity conditions of the optimization problem are provided in Eqs. (26)–(27). Additionally, the complementarity slackness conditions are specified in Eqs. (28)–(31).

$$K^{VPP} + \lambda_1(-I^{VPP} + D^{VPP} - K^{VPP}) + \lambda_2\cdot K^{VPP} + \lambda_3\cdot(-I^{VPP} + L^{VPP,min}) + \lambda_4\cdot(I^{VPP} - L^{VPP,max}) = \Lambda \tag{25}$$

$$\frac{\partial\Lambda}{\partial I^{VPP}} = 0 \rightarrow -\lambda_1 - \lambda_3 + \lambda_4 = 0 \tag{26}$$

$$\frac{\partial\Lambda}{\partial K^{VPP}} = 0 \rightarrow 1 - \lambda_1 - \lambda_2 = 0 \tag{27}$$

$$\lambda_1\cdot(D^{VPP} - I^{VPP} - K^{VPP}) = 0 \tag{28}$$

$$\lambda_2\cdot(K^{VPP}) = 0 \tag{29}$$

$$\lambda_3\cdot(L^{VPP,\min} - I^{VPP}) = 0 \tag{30}$$

$$\lambda_4\cdot(I^{VPP} - L^{VPP,\mathrm{maks}}) = 0 \tag{31}$$

The only way to linearize these equations is by using the big-M formulation. The linearization procedures for the relevant expressions using the M-formulation are provided in Eqs. (33)–(40). Additionally, to satisfy the binary feasibility condition, the non-negativity of the Lagrange multipliers is ensured as described in Eq. (32).

$$\lambda_1, \lambda_2, \lambda_3, \lambda_4 \ge 0 \tag{32}$$

$$\lambda_1 \le u_1^{\mathrm{aux}}\cdot N \tag{33}$$

$$I^{VPP} - D^{VPP} + K^{VPP} \le (1 - u_1^{\mathrm{aux}})\cdot N \tag{34}$$

$$\lambda_2 \le u_2^{\mathrm{aux}}\cdot N \tag{35}$$

$$K^{VPP} \le (1 - u_2^{\mathrm{aux}})\cdot N \tag{36}$$

$$\lambda_3 \le u_3^{\mathrm{aux}}\cdot N \tag{37}$$

$$I^{VPP} - L^{VPP,i} \le (1 - u_3^{\mathrm{aux}})\cdot N \tag{38}$$

$$\lambda_4 \le u_4^{\mathrm{aux}}\cdot N \tag{39}$$

$$-I^{VPP} + L^{VPP,a} \le (1 - u_4^{\mathrm{aux}})\cdot N \tag{40}$$

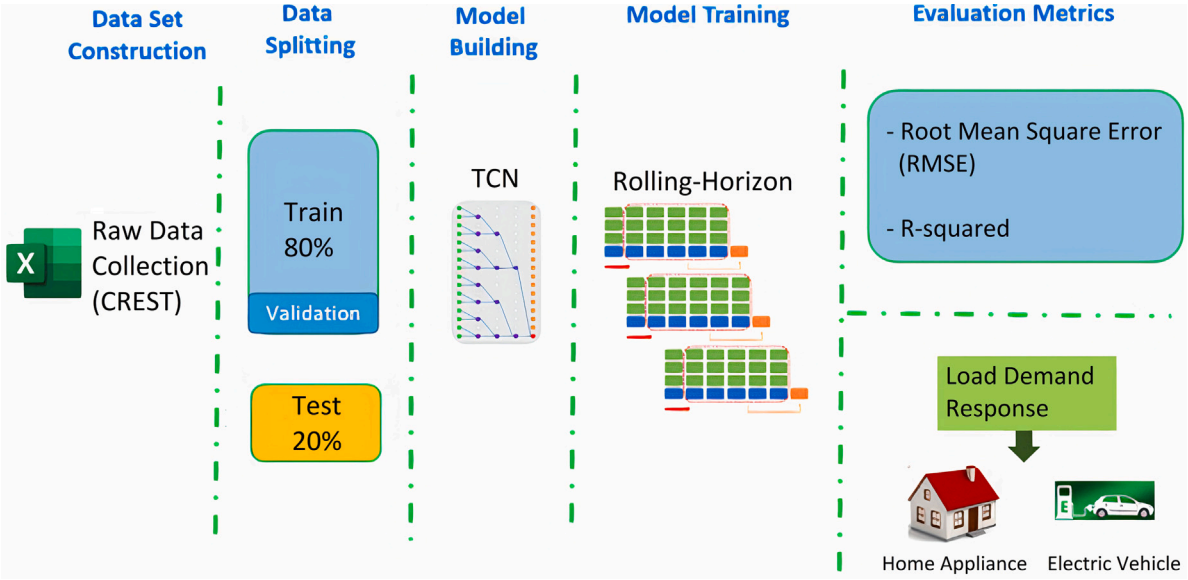


**Fig. 1.** The flow chart of TCN forecasting.

**Table 1**
Configuration and hyperparameters.

| Parameter | Value |
|---|---|
| Input Shape | 5 x 11 |
| Filters | 256 |
| Kernel Size | 2 |
| Stacks | 1 |
| Dilations | 1, 2, 4, 8, 16, 32 |
| Return Sequences | True |
| Activation | ReLu |

**Table 2**
Score comparison of different forecasting models.

| Metric | TCN | LSTM | GRU |
|---|---|---|---|
| R2 | 0.932 | 0.876 | 0.802 |
| RMSE | 366 | 506 | 644 |

### 2.3. TCN based residential load forecasting

In this study, a methodology for forecasting residential load using a TCN (Remy, 2020) is proposed. The TCN is a deep learning model that has proven to be effective in capturing temporal dependencies in time-series data.

The TCN model consists of multiple layers of convolutional and dilated causal convolutional blocks, which allow the model to learn long-term dependencies and patterns in the data. The input to the model is a sequence of past minutely electricity consumptions, and the output is the predicted values for the next sequence. The graphical illustration of TCN model can be seen in Türkoğlu et al. (2024).

Table 1 lists the control hyperparameters and their corresponding values for the TCN model.

## 3. Test and results

This paper first forecasts residential loads using TCN. Then, investigates the impact of EVPL with V2G capability on the DS by employing a MIQCP approach. The proposed model primarily focuses on conducting a comparative analysis of various potential objectives for the distribution system operator. To evaluate the developed strategy, the GurobiPy commercial solver is utilized. The optimization time frame is set to 24 h with a resolution of 15 min.

### 3.1. Residential load forecasting

In this study, the Centre for Renewable Energy Systems Technology (CREST) dataset of minutely electricity consumption from residential buildings over a period of 3000 days, which was collected in its application (Richardson et al., 2008) is used. The data is created to predict short-term time series of residential energy usage which estimates power consumption at a minute resolution based on actual survey data and a probability chain matrix. For this particular model, a three-person family profile is adopted, and monthly data for May profile is generated. In addition to given power demand, CREST residential load generator is used to add realistic household consumption to the predetermined bus.

The CREST dataset consists various type of household appliances with their relevant usage data corresponds to time intervals. It is capable of generating synthetic daily consumption data. 3000 different profiles in order to train TCN model is collected. To prepare the CREST data for modeling, The work first preprocessed it by applying Principal Component Analysis (PCA) to reduce its dimension from 42 to 11. Then the data was sliced into training and validation sets, using an 80/20 ratio. The training set was used to train the TCN model, while the validation set was used to evaluate its performance. Fig. 1 demonstrates the flow chart of the forecasting process that handling the uncertainty related to loads in the study.

The performance of the TCN model using several metrics, root mean squared error (RMSE) and including coefficient of determination (R2) are evaluated. The findings demonstrated that the TCN model has achieved R2 and RMSE score of 0.932 and 366 respectively. The prediction graph and comparison of different forecast scores can be seen in Fig. 2 and Table 2.

### 3.2. V2G enabled bidirectional power flow model in a form of VPP

To verify the optimization model, the IEEE 33-bus (Baran and Wu, 1989) and Midwest US 240-bus distribution test systems (Bu et al., 2019) are employed. EVPLs are placed on Bus-17 for 33-bus system and Bus-130, 150, 190, 230 for 240-bus system respectively. The topology of the IEEE 33 and 240-bus DSs are shown in Fig. 3.

The base power and voltages are configured to be 1 MVA and 12.66 kV/13.8 kV respectively. Algorithm 1 presents the pseudo-code for generating the total active power demands of the entire day from the

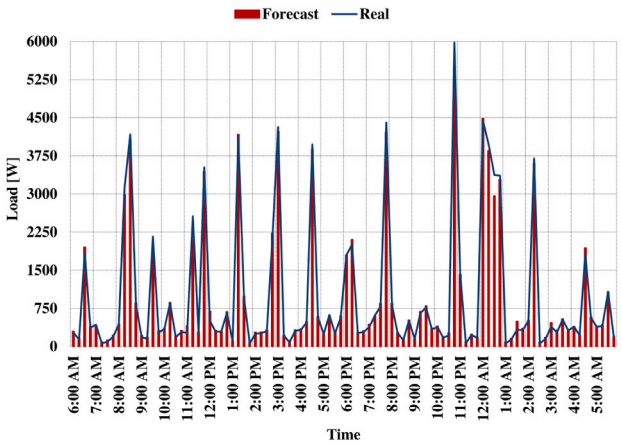


**Fig. 2.** Forecast results of TCN model.

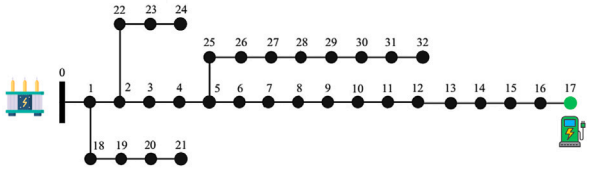

(a) 33-Bus Distribution Test System

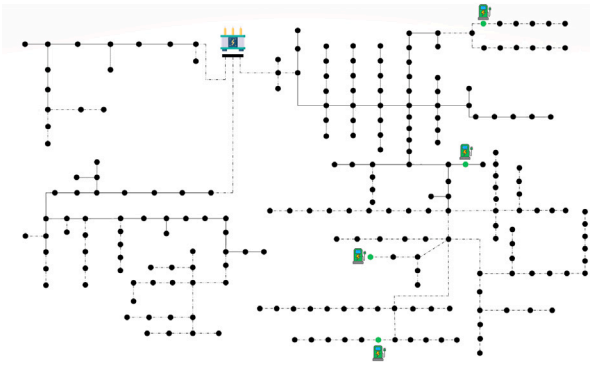

(b) 240-Bus Distribution Test System

**Fig. 3.** IEEE Distribution Test Systems.

relevant IEEE test system documents. For the 240-bus DS, the smart meter data provided by the distributed system operator is employed.

**Algorithm 1** Active/Reactive Demand Generator

1: **for** *iteration* = 1, 2, … 95 **do**
2: **for** *actor* = 1, 2, … , *Bus* **do**
3: Create $T$'th the load value of the $N$'th nus ranging from 0.8 to
4: 1.0 of the original value.
5: **end for**
6: Merge the new load column with the corresponding Bus column
7: **end for**

Price fluctuations are taken from the Germany day-ahead prices from NordPool (Anon, 2023a) and expanded to 15-minute time interval. The 33 and 240-bus power demands and price data are illustrated in Fig. 4.

Lastly, the data of most popular EVs in Europe, 2022 (Peñalver, 2023) was gathered to compile relevant EV dataset such as charge/discharge power, battery capacity, etc. Most selling 50 EVs were selected

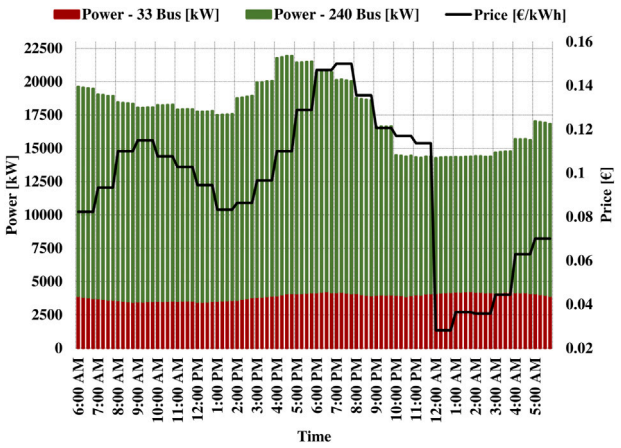


**Fig. 4.** Energy prices and bus loads.

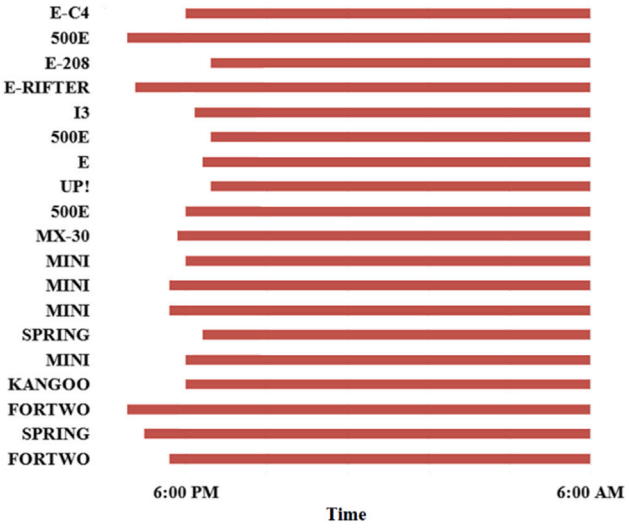


**Fig. 5.** The arrival and departure times of the EVs.

to create an EVPL pool. For the 33-bus and 240-bus DSs, 150 and 750 EVs were randomly selected respectively from the aforementioned list. Since the DS considers residential area, the suitable arrival/departure schedules were generated. Seventy-five percent of the arrival times are randomly distributed within the time frame of 4:30 PM and 7:00 PM. For the departure time, 6:00 AM was selected. The rest of the EVs are regarded as secondary or supplementary automobiles, so they are stationed during the day. Fig. 5 represents sample data from the mentioned EV time intervals.

### 3.3. Simulation and results for the single level problem

To evaluate the model's efficacy, multiple case studies were undertaken, each of which is detailed below:

- Base Case: There are no EVPLs integrated into the DS.

G2V only cases:

- Case-1: Scheduling EVs to minimize total active power loss.
- Case-2: Scheduling EVs to minimize average voltage drop.
- Case-3: Scheduling EVs to maximize total EV profit.

V2G enabled cases:

- Case-4: Scheduling EVs to minimize total active power loss.

**Table 3**
Comparison of the case studies for IEEE 33-Bus.

| Case | Total active power loss [kWh] | Total voltage deviation [pu] | Load factor [%] | Total EV profit [Euro] |
|---|---|---|---|---|
| Base | 3253.956 | 132.7189 | 91.51 | – |
| 1 | 3392.054 | 136.1798 | 91.90 | −137.62 |
| 2 | 3392.492 | 136.1580 | 91.56 | −135.32 |
| 3 | 3536.180 | 136.4818 | 66.93 | −39.55 |
| 4 | 3310.501 | 134.1472 | 91.75 | −58.23 |
| 5 | 3392.298 | 134.0961 | 90.01 | −99.47 |
| 6 | 4717.019 | 140.0293 | 61.87 | 355.89 |

**Table 4**
Comparison of the case studies for Midwest 240-Bus.

| Case | Total active power loss [kWh] | Total voltage deviation [pu] | Load factor [%] | Total EV profit [Euro] |
|---|---|---|---|---|
| Base | 13 047.25 | 1088.297 | 73.64 | – |
| 1 | 13 768.55 | 1116.271 | 75.47 | −612.94 |
| 2 | 13 790.66 | 1116.172 | 75.00 | −654.09 |
| 3 | 13 849.99 | 1116.366 | 76.09 | −339.72 |
| 4 | 13 361.53 | 1109.473 | 74.40 | −506.48 |
| 5 | 13 566.55 | 1107.897 | 74.11 | −445.70 |
| 6 | 14 973.66 | 1131.529 | 70.25 | 934.01 |

- Case-5: Scheduling EVs to minimize average voltage drop.
- Case-6: Scheduling EVs to maximize total EV profit.

The results of the aforementioned scenarios for both the IEEE 33 and 240-bus distribution test systems are illustrated in Tables 3 and 4 respectively. The results reveal that all case studies have higher total active power loss compared to the base case because of the EV loads.

In Table 3, it is noticeable that V2G enabled distribution grid relieves the whole system. When the Case-3 and Case-6 is compared with each other, active power loss increases by 33% due to the arbitrage effects of the EVs. Considering the self-centered actions of EVs', the harmful effect on the network can be easily observed. Any case that EV sell to energy the grid always results with a reduction in their expenses. This indicates that EVs have a substantial influence on line losses and voltage fluctuations. Notably, in Case-6, the findings indicate the highest line losses and expenses, along with the lowest load factor, along with achieving maximum total voltage deviation. When the findings are evaluated based on the load factor, which is a key metric for efficient power system asset utilization, the power loss and voltage deviation cases achieve higher scores rather than the profit cases. The power loss of the Case-4 is 3% lower than the Case 1 since it involves distributed generation thanks to the EVPLs. While Case-3 and Case-6 minimizes the total charging cost, the adverse impacts of EVPL on the grid escalate as line losses increase and the load factor decreases. Nonetheless, the ramp up in the EV expense is trivial when compared to the improvements in grid operation. In Table 4, the base case has the lowest active loss and voltage deviation. In the Midwest 240-bus test system, the case results share similar results. However, it is still clear that the Case-4 and Case-5 demonstrate around 10% better performance in terms of active power loss. In both systems, there is no doubt that V2G-enabled systems can show better efficiency. Also, the EV users spend around 150 Euro less in V2G mode when it is compared with G2V only mode even they are not aimed. Additionally, the Case-6 profits 1270 Euro more than Case-3. Therefore, the proposed models can effectively show the economic benefits of EV charging with the need for efficient power system operation.

Fig. 6 illustrates the allocation of aggregated active power losses among the branches across the various cases for the test systems. The results show that profit-oriented cases exhibit the highest losses in comparison to the other cases during night and result with a nearly 3x and 2x loss in 33 and 240-Bus test systems respectively since EVs prefer to charge for their own benefit. The Case-6 also peaks at noon and valleys at evening differently in both systems. The power loss and voltage deviation minimization cases follow similar trends. The findings suggest that V2G-enabled cases provide the most value as they enable energy trading when the grid is insufficient if their charging behavior is regulated by the grid operator.

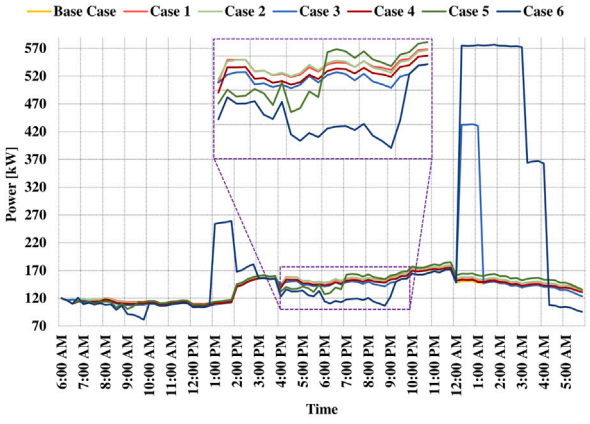


(a) 33-Bus Distribution Test System

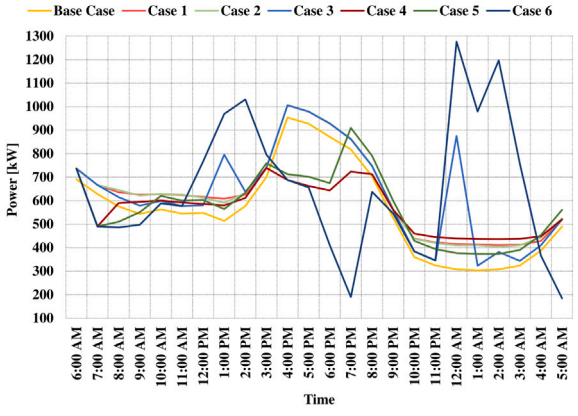


(b) 240-Bus Distribution Test System

**Fig. 6.** Variation of the total line losses with respect to time.

In Fig. 7, the SoE variation of a sample EV parked in EVPL for Case-6 is demonstrated. It is important to note that the EV reaches the desired SoE level of its owner without violating user comfort. However, it should also be clear that in this case, the EV owner only charges or discharges the EV when the electric price is feasible, without

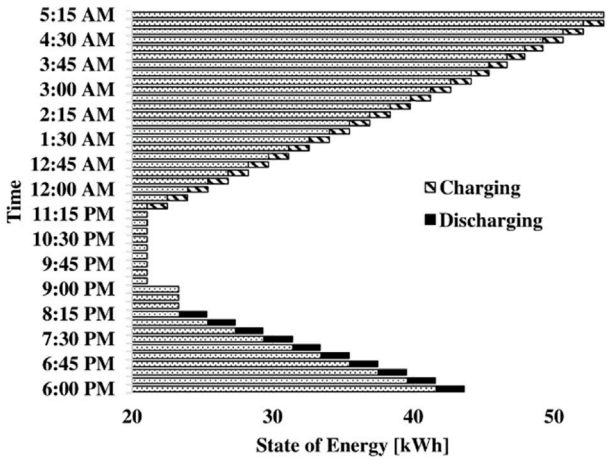


**Fig. 7.** SoE variation of a sample EV.

considering the state of the grid. The EV begin to discharge during evening and assists to the distribution grid until the 9:30 PM as a distributed generator. When the electricity price is low after the 11:30 PM, it starts to charge. Since the minimum, desired and maximum levels of the SoE can be predetermined by the user, this process ensure that the batteries do not exceed the limits.

In Fig. 8, the aggregate power variation of the EVPLs is demonstrated. For Case-4 and Case-5, the EV begins charging when the grid state is feasible, whereas in Case-5, the EV continues discharging to minimize voltage deviation around 6:00PM while Case-4 exhibits more steady pattern. In Case-4 and 5, charging process of the EV appears to be reached peak level in times when an additional distributed generator is needed to stabilize either the power loss or voltage. It is not surprisingly that the Case-4 and 6 follows the reverse pattern with their power loss graphs since EVPL output has inverse effect with the loss. Moreover their power charge–discharge process is same with the electricity price graph in order to maximize their profit. This graphs show that profit-oriented cases can result with an uncontrolled power changes, which is not beneficial for the DS.

The total active power dissipated by the slack bus with respect to time is depicted in Fig. 9. The base case has the smallest generation since there is no additional load on the grid. The Case-1 and Case-2, and Case-4 and Case-5 have same tendency in contrast to the Case-3 and Case-6. In Case-6, it is obvious that V2G reduces the slack bus generation by 4x compared with Case-4 and 5 during evening. But more steady changes are more beneficial like Case-4 and 5 for the DS operator in order to maintain the inertia of the system. Furthermore in the V2G-enabled cases, the slack bus in the 240-bus test system generates 30% less power during midday. It is important that as the EVPLs are placed away from the slack bar, the slack bar generation decreases more since the losses caused by the power transmission is curtailed.

Fig. 10 demonstrates the voltage deviation of the Bus-17 and Bus-230 with respect to time respectively. Since one EVPLs are placed at that buses, the change in the voltage is significant. In Case-6, the EVPL uses all the benefits of the grid by respecting the minimum and maximum voltage levels. When the price is higher at 7:00 PM, the EVs discharge to the grid and the voltage level hits to 1.1 pu. However, when the price decreases at 1:30 AM, the EVs draws from the grid and the voltage level hits to bottom. The Case-3 shows the same trend, but its voltage deviation is not that much since there is no V2G mode. The all-other cases have relatively same attitude, even so Case 4 and 5 accomplish most stable voltage pattern. In base case, the voltage profile is mostly higher since there is not additional EV load. Overall, it is worth to mention that the upper and lower voltage levels are limited

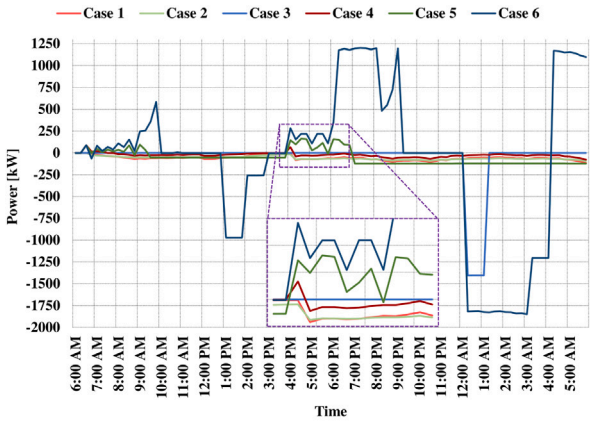


(a) 33-Bus Distribution Test System

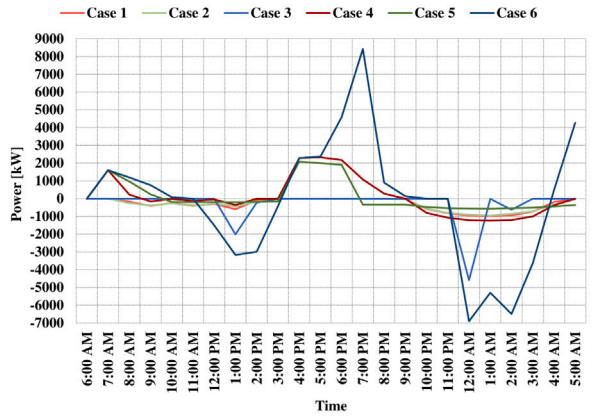


(b) 240-Bus Distribution Test System

**Fig. 8.** Aggregated power variation of the EVPLs.

by the model, and it can result with a much more fluctuation in the real world operations.

The voltage levels of the buses at 12:00 AM for the IEEE 240-Bus distribution test system is shown in Fig. 11. The time slot was specifically chosen because the price signal was at its lowest level, which is likely to encourage charging and increase an additional load demand which nearly peaked even without the EV load. Therefore, this time slot was considered the worst-case scenario. Although the all cases have the same trend, the Case 6 exhibits a better voltage variation. The Case 4 have always lower voltage level for all buses in the 240-bus test system, which is not beneficial for the grid in terms of the voltage profile. However, they can still accomplish both grid's constraints and users' needs. In the 240-Bus test system, the voltage levels are more evident where Base Case has the best profile, followed by power loss and voltage deviation cases which increases system power quality. Nevertheless, EVPL-focused cases loss their advantages and detorate the grid profile.

### 3.4. Simulation and results for the bi-level problem

To demonstrate the efficacy of the bi-level model, different reference values were tried progressively based on $P^{loss}$ minimization and $I^{VPP}$ maximization cases. By examining the balance of $P^{loss}$ and $I^{VPP}$ in the bi-level model according to the different reference values ($D^{VPP}$), the knee point is obtained. The $P^{loss}$ and $I^{VPP}$ balance and knee point line obtained for IEEE 33-Bus distribution test system can be observed in Fig. 12.

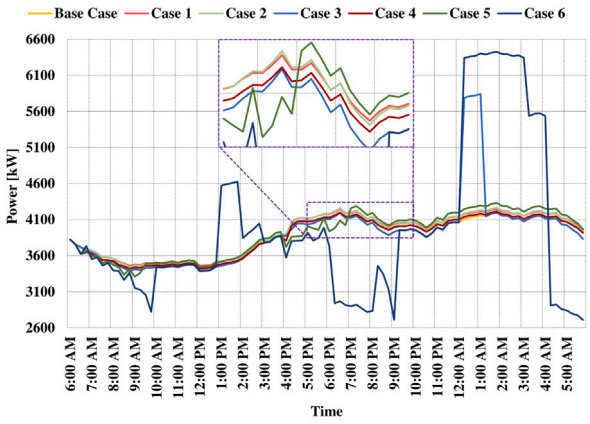


(a) 33-Bus Distribution Test System

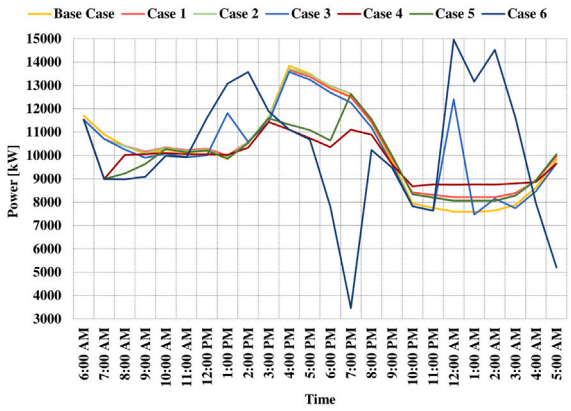


(b) 240-Bus Distribution Test System

**Fig. 9.** Slack bus active power variation.

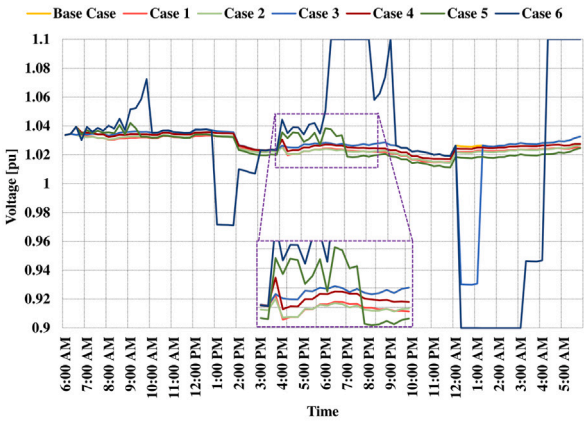


(a) 33-Bus Distribution Test System

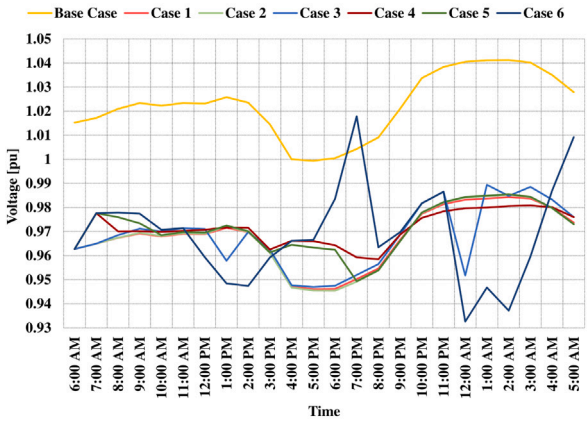


(b) 240-Bus Distribution Test System

**Fig. 10.** Voltage variation of the Bus-17 and Bus-230.

As observed in Fig. 12, initially, significant changes in EVPL gain can be achieved with very small changes in total active power loss in the distribution network. To identify the turning point in this relationship, a knee point analysis was conducted. A knee point is a term used in statistics, particularly in data analysis methods like regression analysis. In this context, the knee point generally represents a point where a straight or curve model transitions to a different curve. This point is where the regression curve begins to deviate from providing a good fit. In regression analysis, this point signifies when the relationship between the dependent variable and the independent variable starts to change, and the model becomes less suitable. According to the results of the relevant bi-level model, a regression analysis was conducted to establish the equation for the curve and subsequently calculate the knee point. The equation that describes the relationship between total active power loss and EVPL gain for the IEEE 33-Bus test system can be seen in Eq. (41) respectively:

$$I^{VPP} = -1.331 \times 10^{14} \cdot \left( \sum_{i,j,t} P_{i,j,t}^{loss} \right)^{-9.7150} + 1.5280 \times 10^{3} \tag{41}$$

Upon examining the relationship between the equations above and Fig. 12, it has been determined that the knee point is located at 3750 kWh of active power loss and 275 Euros of EVPL gain. Based on the knee point, although the break-even point for the sub-level is 275 Euros, two new scenarios were investigated for values of 137.5 Euros and 275 Euros in the upper level, considering the greater importance of power quality in the distribution network.

- Case-7: Bi-level model where reference profit, $D^{VPP}$, is 137.5 Euros
- Case-8: Bi-level model where reference profit, $D^{VPP}$, is 275 Euros

The results of the aforementioned scenarios for the IEEE 33-Bus distribution test system are illustrated in Table 5. When examining Table 5, it is evident that by making only 5% and 14% changes in active power loss, an increase of 196 and 333 Euros in EVPL gain can be achieved, respectively. In contrast, Case-6, results with 43% more loss, but could provide an increase of 408 Euros. This underscores the importance of correctly establishing the balance between the two levels in the bi-level structure. This is because any additional cost beyond the balanced profit of 275 Euros, as achieved in Case-8, results in significantly higher active power loss in the distribution network. Additionally, considering that grid power quality is more important than EVPL gain, it can be foreseen that DSO may choose more balanced profiles such as Case-7.

Fig. 13 represents the total active power loss and voltage deviation for bi-level cases compared to Case-4 and Case-6, respectively. When both Case-7 and Case-8 are examined, it can be seen that they show significant improvements over Case-6, which focuses on EVPL profit maximization. In this regard, while the knee point case may appear relatively worse in terms of voltage, it can be said that it draws a balanced profile, even though voltage deviation minimization is not the primary goal in both levels. However, from the perspective of enhancing grid quality while relatively preserving EVPL gain, Case-7 is considered to be more efficient.

**Table 5**
Comparison of the bi-Level case studies for IEEE 33-Bus.

| Case | Total active power loss [kWh] | Total voltage deviation [pu] | Load factor [%] | Total EV profit [Euro] |
|---|---|---|---|---|
| 4 | 3310.501 | 134.1472 | 91.75 | −58.23 |
| 6 | 4717.019 | 140.0293 | 61.87 | 355.89 |
| 7 | 3468.866 | 135.0582 | 80.18 | 137.5 |
| 8 | 3788.605 | 136.5747 | 72.04 | 275 |

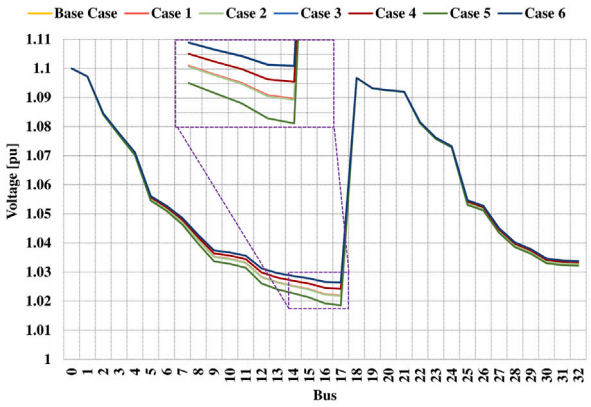


(a) 33-Bus Distribution Test System

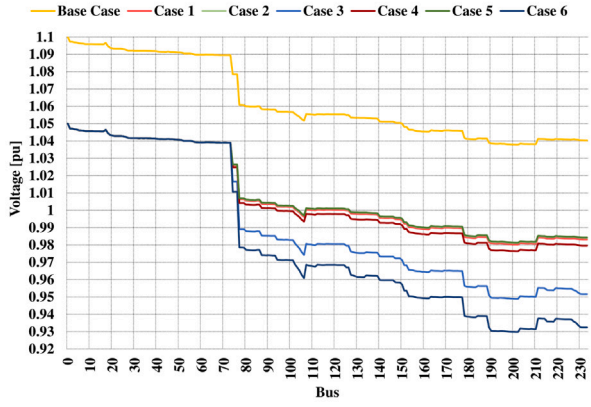


(b) 240-Bus Distribution Test System

**Fig. 11.** Voltage variation of the buses at 12:00 AM.

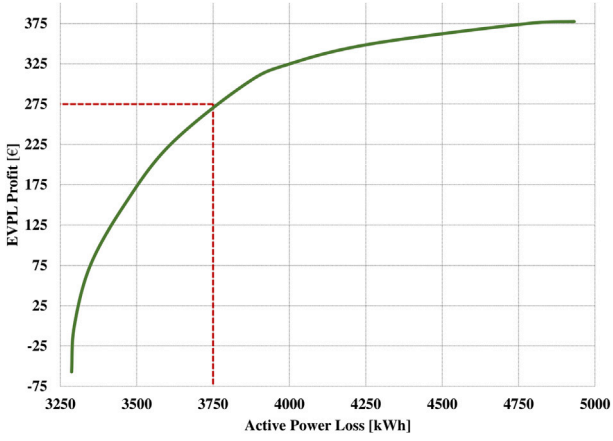


**Fig. 12.** $I^{VPP}$ variation according to different $P^{loss}$ levels.

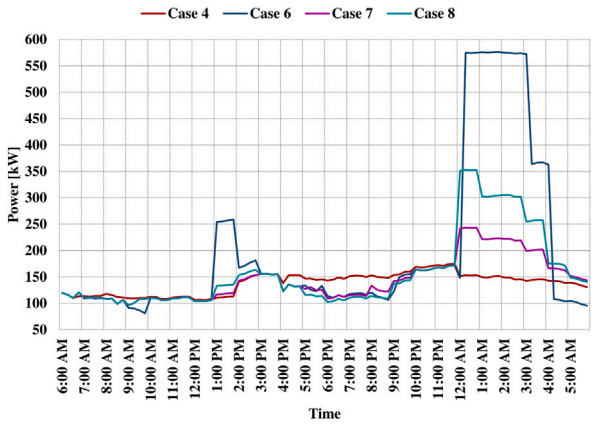


(a) Variation of the total line losses with respect to time.

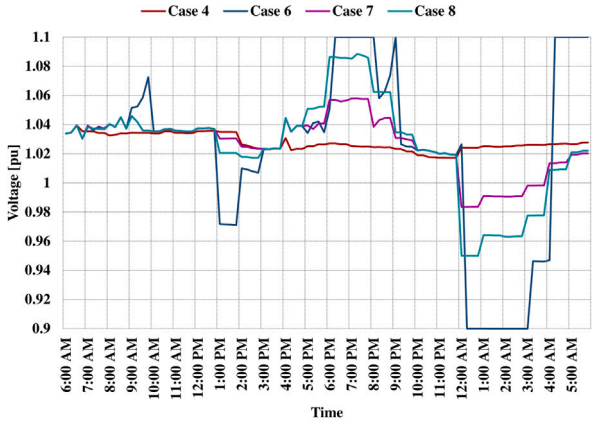


(b) Voltage variation of the Bus-17.

**Fig. 13.** Bi-Level model results.

## 4. Conclusion

As EVs become increasingly popular and the demand for sustainable energy solutions grows, V2G technology is expected to play a crucial role in future energy management. This paper presents a novel EV charging model that considers both grid constraints and EV user preferences, aiming to achieve various objectives from total active power loss minimization to EV profit maximization. Simulations conducted on IEEE 33 and 240-bus DSs demonstrate the effectiveness of the different cases. Results indicate that V2G-enabled models can effectively balance the grid, with Case-4 of the IEEE 33-bus system reducing active power loss by 82 kWh and increasing user profit by 80 Euros compared to Case-1. However, Case-6, despite yielding a 355 Euros user profit, results in unfavorable total active power loss and load factor for the grid. In the IEEE 240-bus system, Cases 4 and 5 achieve better results, with approximately 1500 kWh less active power loss and a 2% improvement in voltage deviation. The study also reveals the significant impact of the bi-level model on EV profit through slight adjustments in active power loss. Moreover, it emphasizes the importance of considering the load factor for efficient power system asset utilization. These findings

offer insights for policymakers and industry professionals seeking to develop sustainable and efficient EV charging solutions. Future research can expand this methodology to larger DSs using smart meter data for improved real-world application accuracy, enabling the identification of system-specific characteristics.

## CRediT authorship contribution statement

**A. Selim Türkoğlu:** Writing – original draft, Visualization, Validation, Methodology, Formal analysis, Data curation, Conceptualization. **H. Cihan Güldorum:** Writing – review & editing, Validation, Methodology, Formal analysis, Conceptualization. **Ibrahim Sengor:** Writing – review & editing, Supervision, Investigation, Funding acquisition. **Alper Çiçek:** Validation, Supervision, Methodology. **Ozan Erdinç:** Validation, Supervision, Project administration, Methodology. **Barry P. Hayes:** Supervision.

## Declaration of competing interest

The authors declare that they have no known competing financial interests or personal relationships that could have appeared to influence the work reported in this paper.

## Data availability

Data will be made available on request.

## References


Aghajan-Eshkevari, S., Ameli, M.T., Azad, S., 2023. Optimal routing and power management of electric vehicles in coupled power distribution and transportation systems. Appl. Energy 341, 121126. http://dx.doi.org/10.1016/j.apenergy.2023.121126.

Ahmed, M., Abouelseoud, Y., Abbasy, N.H., Kamel, S.H., 2021. Hierarchical distributed framework for optimal dynamic load management of electric vehicles with vehicle-to-grid technology. IEEE Access 9, 164643–164658.

Anon, 2023a. Market data, market data | nord pool. [Online]. Available: https://www.nordpoolgroup.com/en/Market-data1/Dayahead/Area-Prices/de-lu/hourly/?view=table. (Accessed 20 February 2023).

Anon, 2023b. Vehicle-to-grid (V2G): Everything you need to know, virta global, 09-jul-2021. [Online]. Available: https://www.virta.global/vehicle-to-grid-v2g. (Accessed: 20 February 2023).

Archana, A.N., Rajeev, T., 2021. A novel reliability index based approach for EV charging station allocation in distribution system. IEEE Trans. Ind. Appl. 57 (6), 6385–6394.

Baran, M.E., Wu, F.F., 1989. Network reconfiguration in distribution systems for loss reduction and load balancing. IEEE Trans. Power Deliv. 4 (2), 1401–1407.

Birk Jones, C., et al., 2022. Impact of electric vehicle customer response to time-of-use rates on distribution power grids. Energy Rep. 8, 8225–8235. http://dx.doi.org/10.1016/j.egyr.2022.06.048.

Bu, F., Yuan, Y., Wang, Z., Dehghanpour, K., Kimber, A., 2019. A time-series distribution test system based on real utility data. In: 2019 North American Power Symposium. NAPS, http://dx.doi.org/10.1109/naps46351.2019.8999982.

Deb, S., Goswami, A.K., Harsh, P., Sahoo, J.P., Chetri, R.L., Roy, R., Shekhawat, A.S., 2020. Charging coordination of plug-in electric vehicle for congestion management in distribution system integrated with Renewable Energy Sources. IEEE Trans. Ind. Appl. 56 (5), 5452–5462.

Dhawale, P.G., Kamboj, V.K., Bath, S.K., Raboaca, M.S., Filote, C., 2024. Integrating renewable energy and plug-in electric vehicles into security constrained unit commitment for hybrid power systems. Energy Rep. 11, 2035–2048. http://dx.doi.org/10.1016/j.egyr.2024.01.027.

Dutta, B., Hwang, H.-G., 2021. Consumers purchase intentions of Green Electric Vehicles: The influence of consumers technological and environmental considerations. Sustainability 13 (21), 12025.

Eid, A., Mohammed, O., El-Kishky, H., 2022. Efficient operation of battery energy storage systems, electric-vehicle charging stations and renewable energy sources linked to distribution systems. J. Energy Storage 55, 105644. http://dx.doi.org/10.1016/j.est.2022.105644.

Guo, Z., Zhou, Z., Zhou, Y., 2020. Impacts of integrating topology reconfiguration and vehicle-to-grid technologies on distribution system operation. IEEE Trans. Sustain. Energy 11 (2), 1023–1032.

Haq, F.U., Bhui, P., Chakravarthi, K., 2022. Real time congestion management using plug in electric vehicles (PEV's): A game theoretic approach. IEEE Access 10, 42029–42043.

Hasanien, H.M., Alsaleh, I., Alassaf, A., Alateeq, A., 2023. Enhanced coati optimization algorithm-based optimal power flow including renewable energy uncertainties and electric vehicles. Energy 283, 129069. http://dx.doi.org/10.1016/j.energy.2023.129069.

Huang, Y., 2019. Day-Ahead Optimal Control of PEV battery storage devices taking into account the voltage regulation of the residential power grid. IEEE Trans. Power Syst. 34 (6), 4154–4167.

IEA, 2022. Global EV Outlook 2022. IEA, Paris, https://www.iea.org/reports/global-ev-outlook-2022. (CC BY 4.0).

Kazemtarghi, A., Dey, S., Mallik, A., 2022. Optimal utilization of bidirectional evs for grid frequency support in power systems. IEEE Trans. Power Deliv. 1–13.

Kwon, S.-Y., Park, J.-Y., Kim, Y.-J., 2020. Optimal V2G and route scheduling of mobile energy storage devices using a linear transit model to reduce electricity and transportation energy losses. IEEE Trans. Ind. Appl. 56 (1), 34–47.

Mazumder, M., Debbarma, S., 2021. Ev charging stations with a provision of V2G and voltage support in a distribution network. IEEE Syst. J. 15 (1), 662–671.

Mehrabi, A., Nunna, H.S., Dadlani, A., Moon, S., Kim, K., 2020. Decentralized greedy-based algorithm for smart energy management in plug-in electric vehicle energy distribution systems. IEEE Access 8, 75666–75681.

Mehta, R., Srinivasan, D., Trivedi, A., Yang, J., 2019. Hybrid planning method based on cost–benefit analysis for smart charging of plug-in electric vehicles in distribution systems. IEEE Trans. Smart Grid 10 (1), 523–534.

Nizami, M.S., Hossain, M.J., Mahmud, K., 2021. A coordinated electric vehicle management system for grid-support services in residential networks. IEEE Syst. J. 15 (2), 2066–2077.

Peñalver, E., 2023. The 50 best selling EV in Europe, EVPlug, 04-Sep-2022. [Online]. Available: https://evplugchargers.com/the-50-best-selling-ev-in-europe/. (Accessed 23 February 2023).

Rajani, B., Kommula, B.N., 2022. An optimal energy management among the electric vehicle charging stations and electricity distribution system using GPC-RERNN approach. Energy 245, 123180. http://dx.doi.org/10.1016/j.energy.2022.123180.

Remy, P., 2020. Temporal Convolutional Networks for Keras. Keras TCN, GitHub.

Richardson, I., Thomson, M., Infield, D., 2008. A high-resolution domestic building occupancy model for energy demand simulations. Energy Build. 40 (8), 1560–1566.

Sengor, I., Guner, S., Erdinc, O., 2020. Real-time algorithm based intelligent EV parking lot charging management strategy providing PLL type demand response program. IEEE Trans. Sustain. Energy 12 (2), 1256–1264.

Singh, J., Tiwari, R., 2020. Cost benefit analysis for V2G implementation of electric vehicles in distribution system. IEEE Trans. Ind. Appl. 56 (5), 5963–5973.

Türkoğlu, A.S., Erkmen, B., Eren, Y., Erdinç, O., Küçükdemiral, İ., 2024. Integrated approaches in resilient hierarchical load forecasting via TCN and optimal valley filling based demand response application. Appl. Energy 360, 122722. http://dx.doi.org/10.1016/j.apenergy.2024.122722.

Velamuri, S., Cherukuri, S.H., Sudabattula, S.K., Prabaharan, N., Hossain, E., 2022. Combined approach for power loss minimization in distribution networks in the presence of gridable electric vehicles and dispersed generation. IEEE Syst. J. 16 (2), 3284–3295.

Wang, F.-P., Yu, J.-L., Yang, P., Miao, L.-X., Ye, B., 2017. Analysis of the barriers to widespread adoption of electric vehicles in Shenzhen China. Sustainability 9 (4), 522.

Zhang, S., Leung, K.-C., 2022. Joint optimal power flow routing and vehicle-to-grid scheduling: Theory and algorithms. IEEE Trans. Intell. Transp. Syst. 23 (1), 499–512.

Zhang, L., et al., 2022. A wind power curtailment reduction strategy using electric vehicles based on individual differential evolution quantum particle swarm optimization algorithm. Energy Rep. 8, 14578–14594. http://dx.doi.org/10.1016/j.egyr.2022.10.442.